International Journal of Automotive Technology, Vol. 12, No. 3, pp. 369–374 (2011)
DOI 10.1007/s12239–011–0043–7

1229–9138/2011/058–07

DRAG REDUCTION OF A PICKUP TRUCK BY A REAR DOWNWARD FLAP

J. HA*, S. JEONG and S. OBAYASHI

Institute of Fluid Science, Tohoku University, Sendai 980-8577, Japan

(Received 8 February 2010; Revised 8 September 2010)

ABSTRACT–The drag reduction of a pickup truck by a rear flap add-on was examined through CFD simulations and wind tunnel experiments. When installed at the rear edge of the roof, the flap increased the cabin back surface pressure coefficient, causing the downwash of the bed flow to be inclined on the tailgate. Thus, the attachment of the bed flow to the tailgate was eliminated; consequently, the drag coefficient was reduced with increasing flap length and downward angle despite the enlarged reverse flow in the wake. However, the drag coefficient did not decrease any further after a specific downward angle was reached because the bed flow increased the drag force at the tailgate and the flap lowered the pressure field above the flap. To maximize the drag reduction effect, the rear downward flap should be designed to have an optimum downward angle.

KEY WORDS : Pickup truck, Drag reduction, Rear flap, Downward angle, Bed flow, Attachment, Tailgate

NOMENCLATURE

C_D : drag coefficient
C_P : pressure coefficient
H : cabin back height
L : vehicle length
Re : Reynolds number
U_∞ : freestream velocity
X, Y, Z : wind tunnel coordinates
l : flap length
θ : downward angle

1. INTRODUCTION

The increasing trend in fuel prices has led to growing concern about vehicle fuel economy. Aerodynamics is one of the most important factors in fuel consumption because an improvement in fuel efficiency can be achieved at a relatively low cost through aerodynamic drag reductions (Jeff, 2002). Thus, a number of wind tunnel tests and computational fluid dynamics (CFD) simulations have been performed to improve the flow characteristics and to reduce the drag coefficients (C_D) of vehicles. The drag coefficient of a typical pickup truck is higher than those of other light vehicles, such as passenger cars or sports utility vehicles (SUVs), which suggests that there is room for improvement in the aerodynamic performance of pickup trucks (Yang and Khalighi, 2005). However, the analysis of the flow field around pickup trucks is difficult because of the open bed behind the cabin. Therefore, most of the previous studies on the aerodynamics of pickup trucks have focused mainly on understanding the flow characteristics around the vehicle.

Al-Garni *et al*. (2003) presented an experimental data set of the flow structure in the near wake region of a generic pickup truck model. They reported that there is a recirculating flow region over the bed bounded by the cab shear layer in the symmetry plane but that there is no such region behind the tailgate. The experimental results were simulated qualitatively by several different computational approaches (Yang and Khalighi, 2005; Lokhande *et al*., 2003; Holloway *et al*., 2009). Mokhtar *et al*. (2009) numerically investigated the effects of the pickup truck configurations on the flow structure around the vehicle and on the generated aerodynamic drag force. The results indicated that a large separation region behind the cabin controls the aerodynamic drag. Cooper (2004) performed full-scale wind tunnel experiments to investigate the aerodynamic effects of the pickup truck tailgate; the results showed that the removal or lowering of the tailgate increases the aerodynamic drag.

Ha *et al*. (2010) carried out an experimental and computational study of the changes in the flow characteristics with variations in the bed geometry of a pickup truck. They found that the bed recirculation flow over the bed and the reverse flow in the wake simultaneously affect the flow characteristics. The bed flow is a recirculation flow over the bed, which is detached from the rear edge of the roof and enters the inside of the bed at the tailgate. The reverse flow in the wake is the same as the wake flow behind the bluff-bodies. They also found that the attachment of the bed flow to the upper part of the tailgate increases the drag

**Corresponding author*. e-mail: ha@edge.ifs.tohoku.ac.jp

coefficient when the bed geometry is unable to cover the downwash of the bed flow entirely. This increase in the drag coefficient can be reduced by increasing either the bed length or the bed height such that the bed flow is not attached to the tailgate. Any modification to the exterior shape, however, may give rise to an increase in the vehicle weight and the high cost and long time required for the vehicle development process.

The objective of this study is to reduce the drag on a pickup truck by adding a rear flap without varying the bed geometry. The use of aerodynamic add-ons is one of the simplest but most effective methods to reduce the drag coefficient; consequently, aerodynamic add-ons have been applied to heavy trucks or bluff-bodies over the past few decades (Kim, 2005; Kim and Youn, 2005; Ortega and Salary, 2004; Khalighi *et al*., 2001). In the case of a pickup truck, however, very few studies have been carried out on the drag reduction with a rear flap add-on. In this study, the rear flap is installed at the rear edge of the roof to secure load performance of the bed. The flap is designed such that it can move downward to control the bed flow; therefore, the bed flow is not attached to the tailgate. The flow characteristics and the drag reduction effect are analyzed by CFD simulations and verified by wind tunnel experiments.

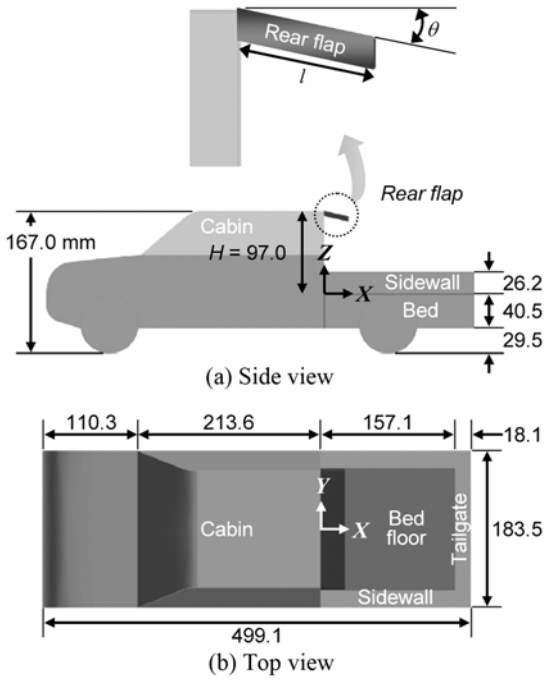

Figure 1. Pickup truck model and rear downward flap.

2. PICKUP TRUCK MODEL

The pickup truck model used was a 1/10th scale generic pickup truck without side mirrors, as shown in Figure 1. The bed length and bed height were 157.1 mm and 26.2 mm, respectively. The most outstanding feature of this bed geometry is the attachment of the bed flow to the tailgate (Ha *et al*., 2010). The flat flap was installed horizontally at the rear edge of the roof without a flap inset. The flap length (l) normalized by the cabin back height (H) and the downward angle (θ) up to 18° were considered as the design variables.

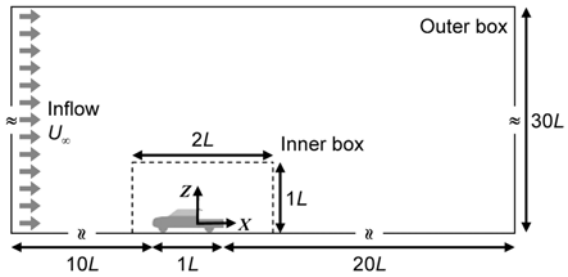

Figure 2. Computational domain of CFD simulations (side view).

3. CFD SIMULATION SETUP

The three-dimensional flow field around the pickup truck model was numerically simulated using Fluent 6.3, a commercial CFD software. This simulation was based on the incompressible steady-state Reynolds-averaged Navier-Stokes (RANS) equations. The turbulence modeling in the current work was carried out using the second-order shear stress transport (SST) k-ω model developed by Menter (1994). This model is a two-equation eddy-viscous model, and it exhibits good behavior in adverse pressure gradients and separating flow conditions.

The computational domain consisted of two boxes: an outer box and an inner box, as shown in Figure 2. The outer box had a length of 10 vehicle lengths (L) in front of the model and 20L behind. The width and height were both 30L to satisfy the freestream condition with zero normal gradients of all flow variables at the side and top faces of the outer box. The inner box was set to control the volume meshes near the model, and it had a length of 2L and a width and height of 1L. The boundary condition of the ground was a stationary wall with the no-slip condition.

The surface and volume meshes were generated by the Gambit program. The model surface was discretized by triangular mesh elements, as shown in Figure 3 (a). To reduce the numerical diffusion and to align with the real flow near the model, the prismatic boundary layers were extruded from the model surface into the computational domain, as shown in Figure 3 (b). Initially, the prisms were grown with a first height of 0.01 mm and a growth factor of 1.2 extruding 17 layers. The remainder of the computational domain was filled with tetrahedral volume cells that were adjacent to the prism layers. The mesh structure was determined by the grid independence test, as shown in Table 1. The test was performed on the basic shape (no flap) model, and the drag coefficient and convergence time

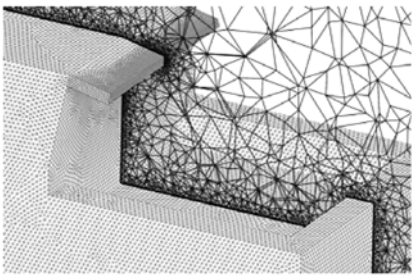

(a) Meshes on the model and in the symmetry plane

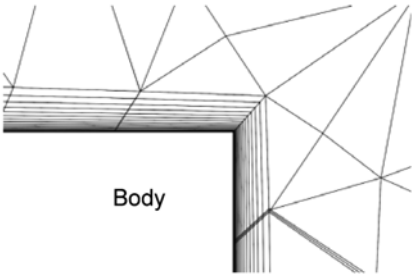

(b) Prismatic boundary layers

Figure 3. CFD mesh configurations.

Table 1. Grid independence test.

Total number of cells	Drag coefficient	Convergence time
Coarse (1.7 million)	0.508	10 h
Medium (2.2 million)	0.505	15 h
Fine 1 (3.0 million)	0.499	24 h
Fine 2 (3.4 million)	0.499	50 h

were selected as the criteria. As the mesh became finer, the drag coefficient converged to 0.499, and the convergence time increased drastically. However, the convergence time of the fine 2 mesh was more than twice that of the fine 1 mesh, although both the fine meshes had the same drag coefficient of 0.499. Thus, the flow field around the pickup truck was simulated with the fine 1 mesh structure.

4. WIND TUNNEL EXPERIMENTAL SETUP

The wind tunnel experiments were conducted in a closed-return, low-turbulence wind tunnel at the Institute of Fluid Science, Tohoku University, as shown in Figure 4. The estimated turbulence intensity of the flow was 0.4%. The freestream velocity (U_∞) was 30 m/s, and the Reynolds number (Re) was 1.03×10^6 based on the overall model length. The exit of the diffuser was octagonal in shape with a subtense length of 420 mm, and the contraction ratio of the diffuser was 12.0. A wooden board was installed at the test section to substitute for the ground. To suppress the separation at the leading edge of the board, the leading edge was formed in an elliptical shape, with an axis ratio of 1/8. The board was 270 mm higher than the bottom of the diffuser to eliminate the effect of the diffuser's boundary layer. The pickup truck model was positioned 280 mm behind the front edge of the board and was lifted up 10 mm by four struts through wheels because the boundary layer thickness of the ground board at the front of the model was 10 mm.

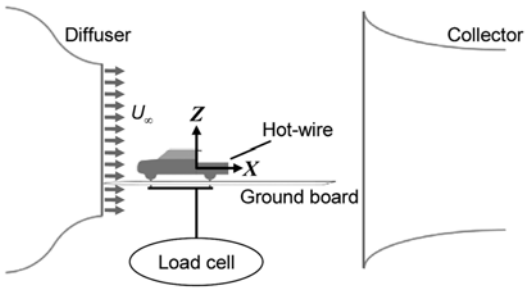

Figure 4. Wind tunnel setup.

The mean drag coefficient was measured by a load cell at a rate of 1,000 Hz for 100 s. The uncertainty of the measured drag coefficients was less than 0.2%. To observe the attachment of the bed flow to the tailgate, the surface flow on the upper surface of the tailgate was visualized by the oil-paint method using a mixture of liquid paraffin and titanium dioxide (TiO_2). The power spectrum density (PSD) in the wake was measured by a single normal hot-wire probe with a frequency response rate of 10 kHz. The measurement point was 15 mm behind the tailgate in the streamwise direction, 70 mm above the bed floor in the symmetry plane ($Y=0$ mm plane).

5. RESULTS AND DISCUSSION

Figure 5 shows the drag coefficient distribution obtained from CFD simulations and wind tunnel experiments involving the flap length and the downward angle. The "△" and "▲" symbols denote the computational and experimental drag coefficients of the basic shape, respectively. Drag coefficients obtained from the CFD simulations were higher than those obtained from the experiments at the non-downward flap ($\theta=0^\circ$), but they were lower than the experimental results at the downward flaps. The discrepancy between the calculated and measured results could be attributed to the steady-state CFD simulations, which were limited to reflecting the unsteady flow characteristics of pickup trucks. However, the maximum error in this case of the two methods was found to be only 1.6%, and the important qualitative trends were the same. A minimum drag coefficient at a downward angle of 12° for all flap lengths was observed with both the methods.

The drag coefficient was reduced with increasing flap length. The rear flap add-on increased the cabin back surface pressure coefficient in the symmetry plane, as shown in Figure 6. When a rear flap add-on was used, the pressures above 0.5 Z/H were higher than that for the basic shape. The rear flap moved the position of the attachment of the bed flow in the downstream direction, as shown in

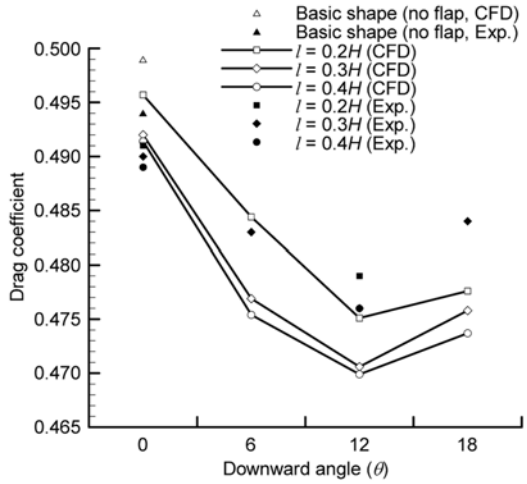

Figure 5. Drag coefficient distribution.

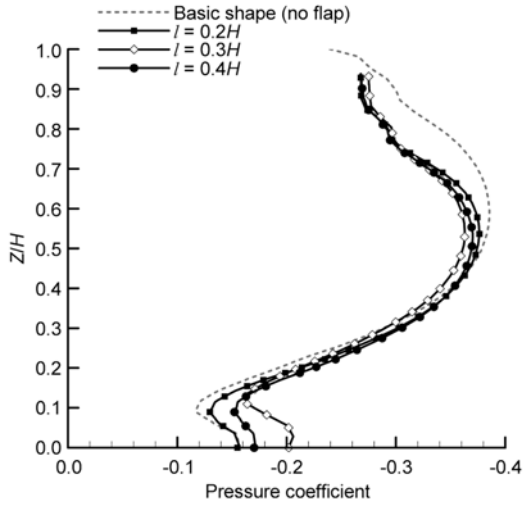

Figure 6. Cabin back surface pressure coefficient distribution in the symmetry plane (downward angle = 0°).

Figure 7 (c). This displacement can also be seen in Figure 8 (b). In comparison to Figure 8 (a), the center of the dispersed flow was shifted to the outer edge of the tailgate. The displaced attachment enabled more downwash of the bed flow to fall into the wake, and thus the size of the reverse flow in the wake was reduced. Thus, the drag coefficients with flap lengths of 0.3H and 0.4H were lower than those with a flap length of 0.2H, in spite of the similar cabin back surface pressure coefficient distribution.

With an increase in the downward angle, the drag coefficient was reduced further. The fact that the bed flow was not attached to the tailgate was responsible for this reduction. The downwash of the bed flow on the tailgate was inclined, as shown in Figure 7 (d) and (e), because the downward flap caused the bed flow to be directed toward the tailgate directly. The core of the bed flow was lowered below 0.5Z/H, and the size of the bed flow became smaller.

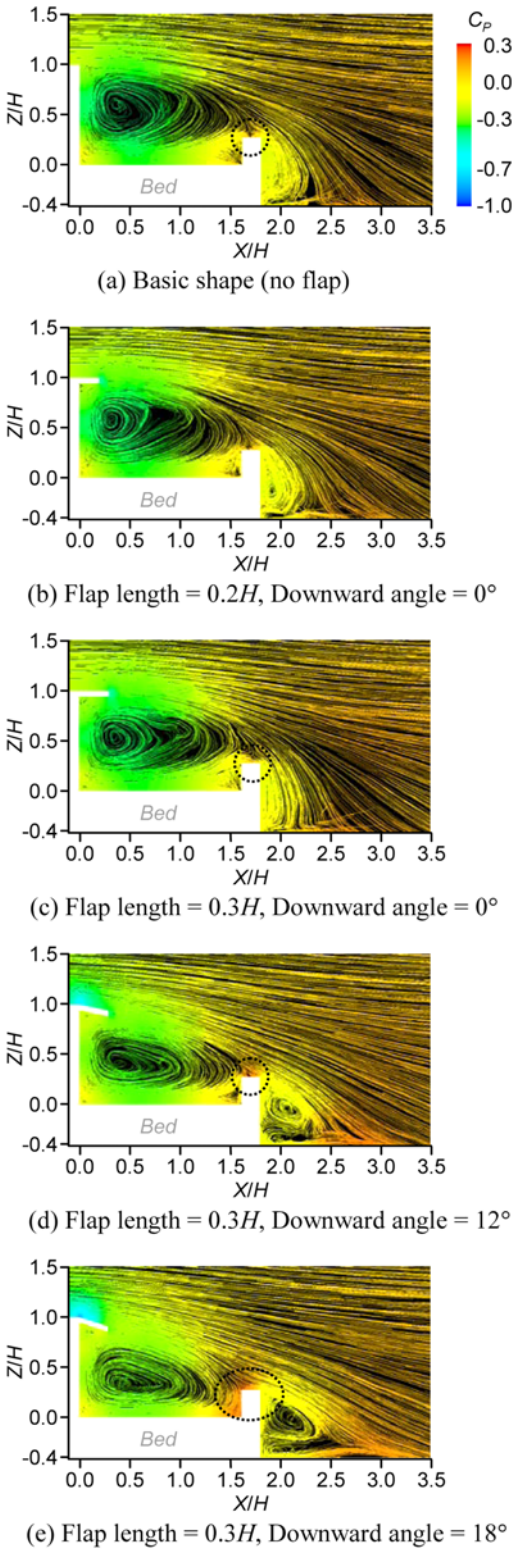

Figure 7. Streamlines colored by the pressure coefficient around the bed in the symmetry plane (CFD data).

Thus, the effect of the bed flow on the tailgate was lessened, and the drag coefficient decreased even though

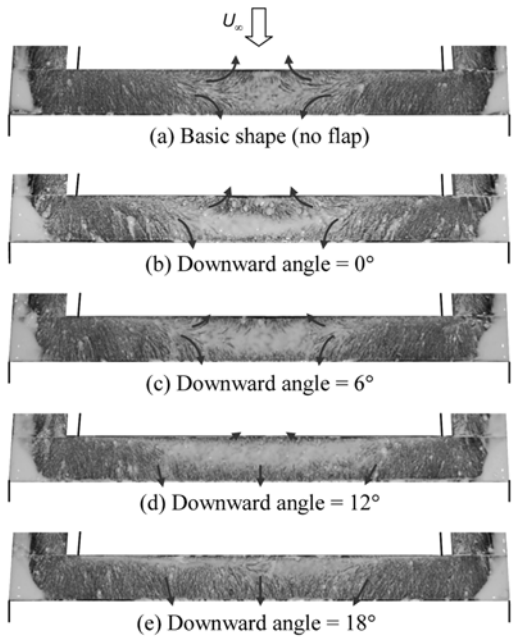

Figure 8. Surface flow visualization on the tailgate (flap length = 0.3H).

the reverse flow in the wake was enlarged.

Figure 8 clearly shows the change in the attachment of the bed flow. The surface flow on the tailgate of the basic shape was dispersed because of the attachment of the bed flow, as shown in Figure 8 (a). However, the dispersed surface flow disappeared as the downward angle increased, as shown in Figure 8 (d) and (e). The disappeared attachment can also be seen from the PSD variation in the wake (Figure 9). The basic shape had a single spectral peak and the largest PSD variation. However, the magnitude of the peak and PSD variation became smaller with increasing downward angle.

The second reason was the increased cabin back surface

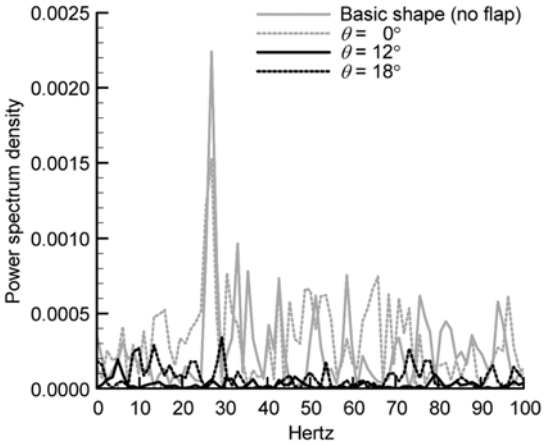

Figure 9. Power spectrum density variation in the wake (flap length = 0.3H).

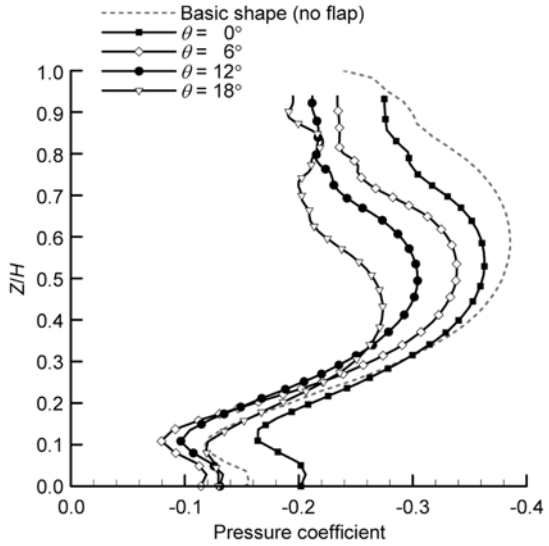

Figure 10. Cabin back surface pressure coefficient distribution in the symmetry plane (flap length = 0.3H).

Table 2. Detailed drag coefficient distribution regarding the downward angle (CFD data, flap length = 0.3H).

	Total C_D	$C_{D\_\text{Cabin back surface}}$	C_{D_Tailgate}	$C_{D\_\text{Cabin body}}$
Basic shape	0.499	0.188	0.055	0.257
$\theta = 0^o$	0.492	0.173	0.056	0.273
$\theta = 12^o$	0.471	0.140	0.056	0.275
$\theta = 18^o$	0.477	0.124	0.070	0.282

pressure coefficient, as shown in Figure 10. As the downward angle increased, the cabin back surface pressure coefficient above 0.35Z/H increased, and the vertical position of the lowest peak was lowered. Therefore, the drag coefficient at the cabin back surface ($C_{D\_\text{Cabin back surface}}$) decreased with increasing downward angle, as shown in Table 2.

The drag reductions by using a flap length of 0.3H and a downward angle of 12° were 0.028 (CFD, 5.6% improvement over that achieved with the basic shape) and 0.018 (Exp., 3.6% improvement). Accordingly, the attachment of the bed flow to the tailgate was eliminated and the cabin back surface pressure increased as the downward angle increased, which in turn reduced the drag coefficient.

The drag coefficient, however, did not decrease further beyond a downward angle of 12° because of the increase in the pressure drag force at the tailgate and the lowered pressure field above the downward flap. The pressure field inside the tailgate with a downward angle of 18° was higher than those of other downward flaps, as shown in Figure 7 (e). Thus, the difference in the pressure within the tailgate and the outside the tailgate increased, which resulted in an increase in the drag force at the tailgate. The drag coefficient at the tailgate (C_{D_Tailgate}) with a downward angle

of 18° increased to as much as 0.070, while those of the other flaps were constant at 0.056, as shown in Table 2, because the rear flap with a downward angle of 18° led the bed flow within the interior of the tailgate, which raised the pressure inside the tailgate. Therefore, the drag coefficient at the tailgate with a downward angle of 18° was the highest.

In addition, the pressure field above the rear flap with a downward angle of 18° was lower than that above the non-downward flap, as shown in Figure 7 (c) and (e) because the flow channel above the flap was expanded by the downward flaps. Thus, the drag coefficient at the cabin body ($C_{D\_\text{Cabin body}}$) with a downward angle of 18° increased to 0.282, as shown in Table 2. The increase in the drag coefficient at the tailgate and at the cabin body offset the drag reduction from the higher cabin back surface pressure coefficient. Therefore, the total drag coefficient with a downward angle of 18° was higher than that with a downward angle of 12°. Accordingly, there exists an optimum downward angle for the lowest drag coefficient.

6. CONCLUSION

The drag reduction of a pickup truck by a rear downward flap was examined computationally and experimentally. The rear downward flap was effective in reducing the drag coefficient through an increase in the flap length and the downward angle. The longer flap increased the cabin back surface pressure coefficient and displaced the attachment of the bed flow in the streamwise direction, which in turn reduced the size of the reverse flow in the wake. The drag coefficient was reduced further with increasing downward angle. The downward flap also increased the cabin back surface pressure coefficient, causing the bed flow to get directed toward the tailgate so that the attachment of the bed flow to the tailgate was eliminated. The surface flow on the tailgate was not dispersed, the power spectrum density in the wake did not consist of a single dominant peak, and the PSD variation became smaller. Therefore, the drag coefficient was reduced even though the reverse flow in the wake was enlarged. The drag reductions obtained by using a flap length of 0.3H and a downward angle of 12° were 0.028 (CFD, 5.6% improvement over that achieved with the basic shape) and 0.018 (Exp., 3.6% improvement).

However, the drag coefficient was not reduced further when the downward angle increased to more than 12°. The bed flow descended further within the tailgate and increased the pressure inside the tailgate, which increased the difference between the pressure within and that outside the tailgate, leading to an increase in the drag coefficient at the tailgate. Moreover, the pressure field above the downward flap was lowered due to the expansion of the flow channel, leading to an increase in the drag coefficient at the cabin body. Hence, the total drag coefficient increased despite the higher cabin back surface pressure coefficient.

In conclusion, the rear downward flap of a pickup truck plays a significant role in reducing the drag coefficient and therefore should be designed at the optimum downward angle to maximize the drag reduction.

REFERENCES

Al-Garni, A. M., Bernal, L. P. and Khalighi, B. (2003). Experimental investigation of the near wake of a pick-up truck. *SAE Paper No*. 2003-01-0651.

Cooper, K. R. (2004). Pickup truck aerodynamics – keep your tailgate up. *SAE Paper No*. 2004-01-1146.

Ha, J., Jeong, S. and Obayashi, S. (2010). Flow characteristics of a pickup truck with regard to the bed geometry variation. *Proc. Inst. Mech. Eng. D, J. Automobile Engineering*, **224**, 881–891.

Holloway, S., Leylek, J. H., York, W. D. and Khalighi, B. (2009). Aerodynamics of a pickup truck: Combined CFD and experimental study. *SAE Int. J. Commercial Vehicles*, **2**, 88–100.

Jeff, H. (2002). Aerodynamic drag of a compact SUV as measured on-road and in the wind tunnel. *SAE Paper No*. 2002-01-0529.

Khalighi, B., Zhang, S., Koromilas, C., Balkanyi, S. R., Bernal, L. P., Laccarino, G. and Moin, P. (2001). Experimental and computational study of unsteady wake flow behind a bluff body with a drag reduction device. *SAE Paper No*. 2001-01-1042.

Kim, M. (2005). Aerodynamic simulation on the drag reduction device of a large-sized bus model. *Int. J. Heavy Vehicle Systems*, **12**, 207–224.

Kim, C. H. and Youn, C. B. (2005). Aerodynamic effect of roof-fairing system on a heavy-duty truck. *Int. J. Automotive Technology* **6**, **3**, 221–227.

Lokhande, B., Sovani, S. and Khalighi, B. (2003). Transient simulation of the flow field around a generic pickup truck. *SAE Paper No*. 2003-01-1313.

Menter, F. R. (1994). Two-equation eddy-viscosity turbulence models for engineering applications. *AIAA J.*, **32**, 1588–1605.

Mokhtar, W. A., Britcher, C. P. and Camp, R. E. (2009). Further analysis of pickup trucks aerodynamics. *SAE Paper No*. 2009-01-1161.

Ortega, J. M. and Salari, K. (2004). An experimental study of drag reduction devices for a trailer underbody and base. *Proc. 34th AIAA Fluid Dynamics Conf. and Exhibit*, AIAA-2004-2252.

Yang, Z. and Khalighi, B. (2005). CFD simulations for flow over pickup trucks. *SAE Paper No*. 2005-01-0547.